European Journal of Pharmaceutics and Biopharmaceutics 136 (2019) 120–130

Contents lists available at ScienceDirect

European Journal of Pharmaceutics and Biopharmaceutics

journal homepage: www.elsevier.com/locate/ejpb

Research paper

Oral coadministration of elacridar and ritonavir enhances brain accumulation and oral availability of the novel ALK/ROS1 inhibitor lorlatinib

Wenlong Li[a], Rolf W. Sparidans[b], Yaogeng Wang[a], Maria C. Lebre[a], Jos H. Beijnen[a,b,c], Alfred H. Schinkel[a,*]

[a] The Netherlands Cancer Institute, Division of Pharmacology, Plesmanlaan 121, 1066 CX Amsterdam, the Netherlands
[b] Utrecht University, Faculty of Science, Department of Pharmaceutical Sciences, Division of Pharmacoepidemiology & Clinical Pharmacology, Universiteitsweg 99, 3584 CG Utrecht, the Netherlands
[c] The Netherlands Cancer Institute/Slotervaart Hospital, Department of Pharmacy & Pharmacology, Plesmanlaan 121, 1066 CX Amsterdam, the Netherlands

ARTICLE INFO

Keywords:
Lorlatinib
Cytochrome P450-3A
Oral bioavailability
Ritonavir
P-glycoprotein
Oatp1a/1b

ABSTRACT

Lorlatinib, a novel generation oral anaplastic lymphoma kinase (ALK) and ROS1 inhibitor with high membrane and blood-brain barrier permeability, recently received accelerated approval for treatment of *ALK*-rearranged non-small-cell lung cancer (NSCLC), and its further clinical development is ongoing. We previously found that the efflux transporter P-glycoprotein (MDR1/ABCB1) restricts lorlatinib brain accumulation and that the drug-metabolizing enzyme cytochrome P450-3A (CYP3A) limits its oral availability. Using genetically modified mouse models, we investigated the impact of targeted pharmacological inhibitors on lorlatinib pharmacokinetics and bioavailability. Upon oral administration of lorlatinib, the plasma $AUC_{0\text{-}8h}$ in CYP3A4-humanized mice was ~1.8-fold lower than in wild-type and *Cyp3a*$^{-/-}$ mice. Oral coadministration of the CYP3A inhibitor ritonavir caused reversion to the $AUC_{0\text{-}8h}$ levels seen in wild-type and Cyp3a$^{-/-}$ mice, without altering the relative tissue distribution of lorlatinib. Moreover, simultaneous pharmacological inhibition of P-glycoprotein and CYP3A4 with oral elacridar and ritonavir in CYP3A4-humanized mice profoundly increased lorlatinib brain concentrations, but not its oral availability or other relative tissue distribution. Oral lorlatinib pharmacokinetics was not significantly affected by absence of the multispecific Oatp1a/1b drug uptake transporters. The absolute oral bioavailability of lorlatinib over 8 h in wild-type, *Cyp3a*$^{-/-}$, and CYP3A4-humanized mice was 81.6%, 72.9%, and 58.5%, respectively. Lorlatinib thus has good oral bioavailability, which is markedly restricted by human CYP3A4 but not by mouse Cyp3a. Pharmacological inhibition of CYP3A4 reversed these effects, and simultaneous P-gp inhibition with elacridar boosted absolute brain levels of lorlatinib by 16-fold without obvious toxicity. These insights may help to optimize the clinical application of lorlatinib.

1. Introduction

Lung cancer is the leading cause of cancer death worldwide, with non-small cell lung cancer (NSCLC) being the predominant form [1,2]. The identification of anaplastic lymphoma kinase (ALK) gene rearrangement as a promising molecular target for treatment heralded a new era of molecular therapy for NSCLC [3,4]. Several ALK inhibitors were developed and applied in the clinic, including crizotinib, ceritinib, alectinib and brigatinib [5–8]. However, most *ALK*-positive tumors eventually become resistant to these drugs through, for instance, secondary *ALK* kinase domain mutations, *ALK* gene amplification, intracellular bypass signaling via EGFR, KIT, SRC, or IGF-1R, disease progression in the brain, and/or pharmacological resistance due to suboptimal central nervous system (CNS) distribution of the drugs [9–13].

Abbreviations: ABC, ATP-binding cassette; ALK, anaplastic lymphoma kinase; ANOVA, analysis of variance; AUC, area under plasma concentration-time curve; BBB, blood-brain barrier; BCRP, breast cancer resistance protein; C_{brain}, brain concentration; C_{max}, maximum drug concentration in plasma; C_{testis}, testis concentration; CNS, central nervous system; CYP, Cytochrome P450; Cyp3a$^{-/-}$, Cyp3a knockout mice; Cyp3aXAV, Cyp3a knockout mice with specific expression of human CYP3A4 in liver and intestine; LC-MS/MS, liquid chromatography coupled with tandem mass spectrometry; NSCLC, non-small cell lung cancer; P-gp, P-glycoprotein; SD, standard deviation; T_{max}, time to reach maximum drug concentration in plasma

* Corresponding author at: Division of Pharmacology, The Netherlands Cancer Institute, Plesmanlaan 121, 1066 CX Amsterdam, the Netherlands.
E-mail address: a.schinkel@nki.nl (A.H. Schinkel).

https://doi.org/10.1016/j.ejpb.2019.01.016
Received 24 October 2018; Received in revised form 9 January 2019; Accepted 16 January 2019
Available online 17 January 2019
0939-6411/

The potential importance of CNS penetration of the drugs was further suggested by Gadgeel et al., who found in an alectinib study that *ALK*-positive NSCLC shows a high prevalence of brain/meningeal disease of up to 40% at diagnosis, which further increased during treatment [14].

Lorlatinib (PF-06463922), a third-generation ALK inhibitor, was developed utilizing structure-based drug design, lipophilic efficacy and physical-property-based optimization (Supplemental Fig. 1) [15]. This unique macrocyclic ALK inhibitor possesses significantly increased lipophilic efficacy and showed broad-spectrum potency and desirable absorption, distribution, metabolism, and excretion properties, including CNS availability. Moreover, lorlatinib shows promising activity against *ALK*-rearranged tumors *in vitro* and in clinical trials [16,17]. Importantly, lorlatinib was highly active in the CNS, inducing intracranial responses in 42% and 60% of *ALK*-positive and *ROS1*-positive patients with baseline measureable CNS disease, respectively [18]. Moreover, the promising intracranial activity of lorlatinib was further confirmed in a recent global phase 2 study with 63% objective intracranial responses in *ALK*-positive patients [19].

Using genetically modified cell lines and mouse models, we recently demonstrated that P-glycoprotein (P-gp) limits the brain accumulation of lorlatinib without affecting lorlatinib oral plasma exposure, and that CYP3A restricts its systemic exposure [20]. Otherwise very little is currently known about lorlatinib metabolism based on publicly available data. P-gp is a member of the ATP-binding cassette efflux transporter family expressed in multiple tissues, such as liver, kidney, intestine, as well as BBB [21,22]. Members of the CYP superfamily of enzymes are responsible for most phase I drug metabolism [23]. Many drugs are metabolized by CYP3A4/5, the most abundant CYP enzymes in human liver and intestine, leading to either inactivation or sometimes activation [24]. We previously found that knockout of the Cyp3a gene resulted in 1.3-fold increased plasma exposure of lorlatinib, which was then 2-fold reduced by transgenic overexpression of human CYP3A4 in liver and intestine, without affecting the relative tissue distribution of lorlatinib. This suggests that human CYP3A4 limits systemic exposure of lorlatinib more efficiently than the mouse Cyp3a enzyme [20].

In view of the potential benefits of further enhancing lorlatinib brain accumulation to better treat brain metastases or of enhancing lorlatinib oral availability, the use of targeted pharmacological inhibitors of drug transporters and drug-metabolizing enzymes can be considered. Therefore, a promising strategy to boost the brain distribution and systemic exposure of lorlatinib would be to combine oral formulations of lorlatinib with inhibitors elacridar or ritonavir alone, or a combination of both. We previously studied the effects of elacridar, a strong ABCB1/ABCG2 inhibitor, on pharmacokinetics and tissue distribution of lorlatinib [20]. We found that concomitant administration of elacridar to wild-type mice increased the brain-to-plasma ratio of lorlatinib 4.0-fold, to levels similar to those seen in the *Abcb1a/1b;Abcg2*$^{-/-}$ mice, without altering the systemic exposure of lorlatinib.

The HIV protease inhibitor ritonavir, a highly efficient CYP3A inhibitor, can boost systemic exposure of many drugs, such as docetaxel, paclitaxel, and lopinavir, by extensive inhibition of CYP3A [25,26]. It is yet unclear whether lorlatinib oral availability could also be substantially increased by coadministration of ritonavir. Moreover, simultaneous inhibition of P-gp and CYP3A by drugs co-administered with orally administered lorlatinib may have the potential benefit of boosting both brain distribution and systemic exposure to enhance the overall therapeutic efficacy of lorlatinib. However, the further increased exposure of lorlatinib in brain and systemic circulation might also result in increased toxicity risks.

In the present preclinical study, we firstly examined whether we could substantially increase oral availability of lorlatinib by inhibition of CYP3A using oral co-administration of ritonavir. We subsequently investigated whether exposure of lorlatinib in brain and systemic circulation could be further safely boosted by the simultaneous inhibition of P-gp and CYP3A with both elacridar and ritonavir. The impact of mouse and human CYP3A4 on oral bioavailability of lorlatinib was also studied and clarified. Finally, in a pilot experiment we assessed a possible role of Oatp1a/1b drug uptake transporters in lorlatinib oral availability and liver distribution.

2. Materials and methods

2.1. Chemicals

Lorlatinib was purchased from TargetMol (Boston, MA, USA). Ritonavir and elacridar HCl were obtained from Sequoia Research Products (Pangbourne, United Kingdom). Bovine Serum Albumin (BSA) Fraction V was obtained from Roche Diagnostics GmbH (Mannheim, Germany). Glucose water (5%, w/v) was supplied by B. Braun Medical Supplies (Melsungen, Germany). Isoflurane was purchased from Pharmachemie (Haarlem, The Netherlands), heparin (5000 IU ml^{-1}) was from Leo Pharma (Breda, The Netherlands). Other chemicals used in the lorlatinib assays were described before [27,28] and all other chemicals and reagents were obtained from Sigma-Aldrich (Steinheim, Germany).

2.2. Animals

Mice were housed and handled according to institutional guidelines complying with Dutch and EU legislation. All experiments were approved by the institutional board for the care and use of laboratory animals. Wild-type, *Cyp3a*$^{-/-}$ and Cyp3aXAV mice [29], all of a > 99% FVB genetic background, were used between 10 and 15 weeks of age. Animals were kept in a temperature-controlled environment with a 12-h light and 12-h dark cycle and received a standard diet (Transbreed, SDS Diets, Technilab – BMI, Someren, The Netherlands) and acidified water *ad libitum*.

2.3. Drug solutions

For oral and intravenous administration, lorlatinib was dissolved in dimethyl sulfoxide (DMSO) at a concentration of 50 mg/ml and further diluted with a mixture of polysorbate 80/ethanol (1:1, v/v), and then 5% (w/v) glucose in water to yield a concentration of 1.0 mg/ml. Final concentrations for DMSO, polysorbate 80, ethanol and glucose in the dosing solution were 2%, 1.5%, 1.5% and 4.75% (v/v/v/w), respectively. Elacridar hydrochloride was dissolved in DMSO (106 mg/ml) in order to get 100 mg elacridar base per ml DMSO. The stock solution was further diluted with a mixture of polysorbate 80, ethanol and water [20:13:67, (v/v/v)] to yield a concentration of 10 mg/ml elacridar, and orally administered at a dose of 100 mg/kg body weight. For the ritonavir boosting experiment, 15 mg/ml ritonavir in polysorbate 80/ethanol (1:1, v/v) was made and stored at −30 °C, which was then further diluted with water (1:5, v/v) to obtain 2.5 mg/ml working solution for administration. To obtain the coadministration formulation for the double-booster experiment, 12.5 mg/ml ritonavir and 56 mg/ml elacridar were dissolved in DMSO, then further diluted with polysorbate 80 and water to yield concentrations of 2.5 mg/ml ritonavir and 10 mg/ml elacridar (final solvent ratios, DMSO: polysorbate 80: water, 1:1:3, v/v/v). All dosing solutions were prepared freshly on the day of experiment.

2.4. Lorlatinib administration schedules with targeted inhibitors

Wild-type, *Cyp3a*$^{-/-}$ and Cyp3aXAV mice were fasted for 3 h before oral drug administration to minimize variation in absorption. Lorlatinib was administered orally at dose of 10 mg/kg, elacridar was administered orally at a dose of 100 mg/kg, and ritonavir was administered orally at 25 mg/kg of bodyweight. Oral administration was performed by gavage into the stomach, using a blunt-ended needle, at 10 µl/g of body weight. In case of coadministration with elacridar, ritonavir or

elacridar and ritonavir, the booster(s) solutions were orally administered 15 min prior to oral lorlatinib administration.

2.5. Lorlatinib administration schedules for oral bioavailability study

Wild-type, *Cyp3a*$^{-/-}$ and Cyp3aXAV mice were fasted for around 3 h before drug administration. Lorlatinib was administered either orally by gavage into the stomach or intravenously into the tail vein, at dosages of 10 mg/kg and 5 mg/kg, respectively.

2.6. Sample collection

For boosting experiments, tail vein blood (~50 µl per sample) sampling was performed at 0.25, 0.5, 1, 2, and 4 h time points after oral administration using microvettes containing heparin.

For the oral bioavailability study, tail vein blood (~50 µl per sample) sampling was performed at 0.125, 0.25, 0.5, 1, 2, and 4 h time points after oral or intravenous administration using microvettes containing heparin.

Eight hours after oral or intravenous administration, mice were anesthetized with isoflurane and blood was collected by cardiac puncture. Blood samples were collected in Eppendorf tubes containing heparin as an anticoagulant. The mice were then sacrificed by cervical dislocation and organs were rapidly removed. The contents of the small intestine were removed, and the tissue quickly rinsed with saline to remove any residual feces before homogenization of the tissue. Plasma was isolated from the blood by centrifugation at 9000*g* for 6 min at 4 °C, and the plasma fraction was collected and stored at −30 °C until analysis. Brain, liver, small intestinal tissue, and testis were weighed and then homogenized with 1, 3, 3, or 1 ml of 4% (w/v) bovine serum albumin, respectively. All samples were stored at −30 °C until analysis.

2.7. Bioanalytical analysis

Lorlatinib concentrations in plasma samples and organ homogenates were determined using sensitive and specific liquid chromatography-tandem mass spectrometry assays [27,28].

2.8. Pharmacokinetic calculations and statistical analysis

The area under the plasma concentration-time curve (AUC) was calculated using the trapezoidal rule, without extrapolating to infinity. The peak plasma concentration (C_{max}) and the time of maximum plasma concentration (T_{max}) were estimated from the original data. The absolute oral bioavailability was calculated as the ratio of the (dose-normalized) plasma $AUC_{0\text{-}8h}$ after oral and intravenous administration. The standard deviation for the oral bioavailability was estimated using the following formulae [30]:

$$CV = SD/Mean$$

$$CVb \cong \sqrt{CVo^2 + CVi^2}$$

where CV*b*, CV*o*, and CV*i* are the coefficients of variation (CV) of oral bioavailability, oral plasma $AUC_{0\text{-}8h}$ and intravenous plasma $AUC_{0\text{-}8h}$, respectively.

Pharmacokinetic parameters were calculated by non-compartmental methods using the software package of PK solutions 2.0.2 (SUMMIT, Research Service, Ashland, OH, USA). One-way analysis of variance (ANOVA) was used when multiple groups were compared and the Bonferroni *post hoc* correction was used to accommodate multiple testing. Tukey's *post hoc* correction was also applied, and yielded essentially identical results. Differences were considered statistically significant when $P < 0.05$. All data are presented as geometric mean ± SD.

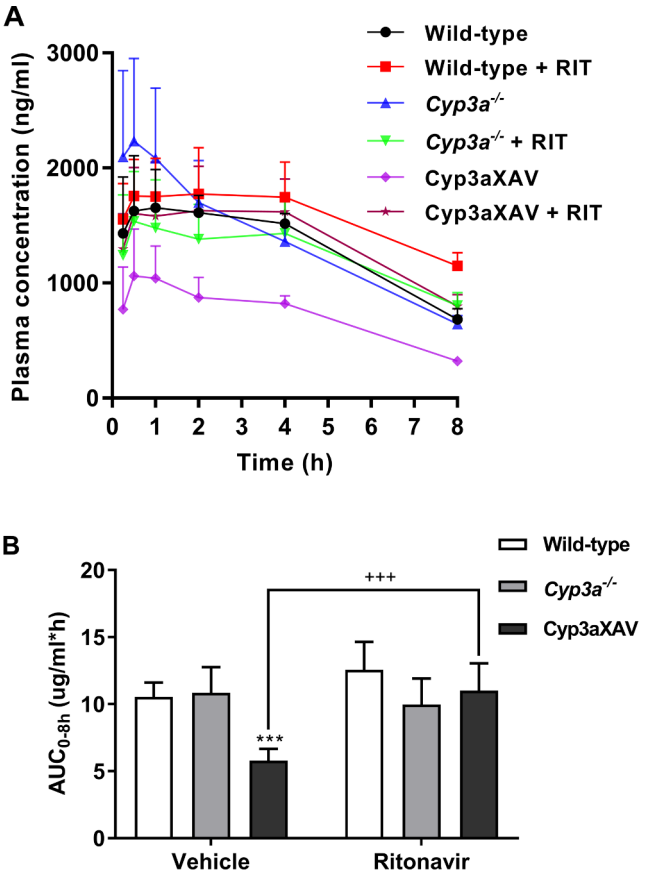

Fig. 1. Plasma concentration-time curves and $AUC_{0\text{-}8h}$ of lorlatinib in male wild-type, *Cyp3a*$^{-/-}$ and Cyp3aXAV mice over 8 h after oral administration of 10 mg/kg lorlatinib (n = 5–7). Vehicle or 25 mg/kg ritonavir was orally administered 15 min prior to lorlatinib administration. Panel A: plasma concentration-time curves of lorlatinib in the mouse strains with or without ritonavir treatment. RIT = ritonavir. Panel B: plasma $AUC_{0\text{-}8h}$ of lorlatinib. *, $P < 0.05$; **, $P < 0.01$; ***, $P < 0.001$ compared to vehicle-treated wild-type mice; $^{+}$, $P < 0.05$; $^{++}$, $P < 0.01$; $^{+++}$, $P < 0.001$ comparing Cyp3aXAV mice with or without ritonavir.

3. Results

3.1. Lorlatinib exposure after coadministration with ritonavir

In order to optimize the pharmacokinetics of lorlatinib and examine whether we could substantially increase the oral availability of lorlatinib by inhibition of CYP3A, we administered ritonavir (25 mg/kg) or vehicle orally 15 min prior to oral lorlatinib (10 mg/kg) to male wild-type, *Cyp3a*$^{-/-}$, and Cyp3aXAV mice. Cyp3aXAV mice are *Cyp3a*$^{-/-}$ mice with transgenic overexpression of human CYP3A4 in liver and intestine (CYP3A4-humanized mice). In vehicle-treated mice, plasma $AUC_{0\text{-}8h}$s were not significantly different between wild-type and *Cyp3a*$^{-/-}$ mice, but they were markedly (1.8-fold) lower in Cyp3aXAV mice (Fig. 1A and B; Table 1). Pretreatment with ritonavir did not result in a significant increase in plasma $AUC_{0\text{-}8h}$ in wild-type or *Cyp3a*$^{-/-}$ mice (Table 1). In contrast, a strong increase (1.9-fold) in the plasma $AUC_{0\text{-}8}$ was observed in Cyp3aXAV mice in the presence of ritonavir, to levels equal to those seen in wild-type and Cyp3a$^{-/-}$ mice (Fig. 1A and B; Table 1).

In the absence of ritonavir, brain-to-plasma ratios of lorlatinib were similar among wild-type, *Cyp3a*$^{-/-}$, and Cyp3aXAV mice (Fig. 2A and B). In contrast to the obvious effects on plasma exposure of lorlatinib, ritonavir had no substantial influence on the brain-to-plasma ratios in these three mouse strains. A similar situation was observed for liver,

Table 1
Plasma, brain and testis pharmacokinetic parameters of lorlatinib over 8 h after oral administration of 10 mg/kg lorlatinib to male wild-type, *Cyp3a*$^{-/-}$ and Cyp3aXAV mice without or with ritonavir coadministration.

Parameter	Genotype and type of pre-treatment					
	Vehicle			Ritonavir		
	Wild-type	*Cyp3a*$^{-/-}$	Cyp3aXAV	Wild-type	*Cyp3a*$^{-/-}$	Cyp3aXAV
AUC_{0-8h}, ng/ml h	10542 ± 1067	10842 ± 1912	5792 ± 871***	12558 ± 2089	9971 ± 1941	11013 ± 2023 $^{+++}$
Fold change AUC_{0-8h}	1.00	1.03	0.55	1.19	0.95	1.04
C_{max}, ng/ml	1654 ± 332	2234 ± 719	1145 ± 327	1774 ± 404	1537 ± 432	1628 ± 386
T_{max}, h	0.5–2.0	0.25–4.0	0.5–4.0	0.5–4.0	0.25–2.0	0.5–4.0
C_{brain}, ng/g	312 ± 44	303 ± 48	150 ± 20***	556 ± 125**	385 ± 73	345 ± 57 $^{+++}$
Fold change C_{brain}	1.00	0.97	0.48	1.78	1.23	1.11
Brain-to-plasma ratio	0.46 ± 0.04	0.47 ± 0.08	0.47 ± 0.05	0.48 ± 0.07	0.48 ± 0.07	0.43 ± 0.06
Fold change ratio	1.00	1.02	1.02	1.04	1.04	0.93
C_{testis}, ng/g	633 ± 85	548 ± 113	250 ± 11***	1049 ± 146***	705 ± 153	750 ± 223 $^{+++}$
Fold change C_{testis}	1.00	0.86	0.40	1.66	1.11	1.12
Testis-to-plasma ratio	0.93 ± 0.10	0.85 ± 0.10	0.79 ± 0.10	0.91 ± 0.09	0.88 ± 0.21	0.94 ± 0.26
Fold change ratio	1.00	0.91	0.81	0.98	0.95	1.01

Data are presented as mean ± S.D. (n = 5–7). Lorlatinib was administered alone or coadministered with 25 mg/kg oral ritonavir 15 min before lorlatinib administration. AUC_{0-8h}, area under plasma concentration–time curve; C_{max}, maximum concentration in plasma; T_{max}, time point (h) of maximum plasma concentration (range for individual mice); $C_{brain/testis}$, brain/testis concentration; $P_{brain/testis}$, brain/testis accumulation. *, $P < 0.05$; **, $P < 0.01$; ***, $P < 0.001$ compared to vehicle-treated wild-type mice; $^{+}$, $P < 0.05$; $^{++}$, $P < 0.01$; $^{+++}$, $P < 0.001$ comparing Cyp3aXAV mice with or without ritonavir treatment.

small intestinal tissue, and testis (Fig. 2C–H; Table 1).

As shown by us previously, these data confirm that transgenic human CYP3A4 has a more substantial impact on lorlatinib pharmacokinetics than endogenous mouse Cyp3a [20]. We now found that oral ritonavir treatment could extensively inhibit the *in vivo* activity of human CYP3A4, leading to markedly increased lorlatinib plasma concentrations and overall tissue exposure in Cyp3aXAV mice. However, mouse and human CYP3A4 activity appeared to have no significant effect on the relative tissue distribution of lorlatinib. Moreover, the lack of effect of ritonavir on lorlatinib exposure in the *Cyp3a*$^{-/-}$ mice suggests that no other lorlatinib-metabolizing enzymes (or lorlatinib transporters, for that matter) were noticeably affected by ritonavir at this dose (Figs. 1 and 2; Table 1).

3.2. Lorlatinib exposure after combined coadministration of elacridar and ritonavir

To further investigate to what extent we could enhance plasma and brain exposure of lorlatinib by simultaneous pharmacological inhibition of P-gp and CYP3A, we performed a double-boosting experiment. Based on the ritonavir boosting experiment described above, there is a species difference for lorlatinib in CYP3A substrate specificity or enzyme activity between endogenous mouse Cyp3a and human CYP3A4. We therefore used Cyp3a knockout mice with specific expression of human CYP3A4 in liver and intestine to better model the human CYP3A4 situation in lorlatinib metabolism. We observed a 2.0-fold increase in plasma AUC_{0-8h} of lorlatinib in mice with coadministration of combined elacridar and ritonavir compared to vehicle-treated mice (Fig. 3; Table 2), but this increased plasma exposure of lorlatinib was not significantly higher than that in mice with coadministration of ritonavir alone (Table 2; $P > 0.05$). Moreover, in elacridar-cotreated mice, the lorlatinib plasma AUC_{0-8h} was not significantly different from that in vehicle-treated mice. These data suggest that elacridar did not significantly affect the oral availability of lorlatinib, consistent with what we previously observed in a 2 h elacridar/lorlatinib boosting experiment [13]. The increase after the chemical inhibition with ritonavir was clear and comparable to the increase in oral AUC_{0-8h} in the complete absence of mouse Cyp3a and human CYP3A4 (compare Fig. 3 and Table 2 with Fig. 1 and Table 1). These data therefore suggest that for lorlatinib in transgenic mice, the inhibition of intestinal and hepatic CYP3A4 by ritonavir was virtually complete.

In single elacridar-cotreated Cyp3aXAV mice, the brain concentrations were markedly increased by 8.1-fold compared to vehicle-treated mice, which could be further increased by additional coadministration of ritonavir to 16.4-fold higher absolute brain concentrations (Fig. 4A; Table 2). Correcting for the increased plasma levels due to the boosting agents (primarily ritonavir), lorlatinib brain-to-plasma ratios were substantially increased by 3.8-fold and 4.3-fold in Cyp3aXAV mice upon coadministration of elacridar alone or elacridar and ritonavir combined, respectively (Fig. 4B; Table 2). Qualitatively similar results were obtained for testis (Fig. 4G and H; Table 2). In contrast, lorlatinib relative tissue distribution in the liver and small intestinal tissue was not noticeably altered by coadministration of either elacridar alone or elacridar plus ritonavir (Fig. 4C–F).

Collectively, the data indicate that elacridar had no noticeable effects on boosting oral availability or plasma exposure of lorlatinib, but could substantially increase lorlatinib distribution into the brain and testis, both in the absence and presence of ritonavir boosting. Oral coadministration of elacridar and ritonavir did not substantially further increase either plasma exposure of lorlatinib compared to single ritonavir-treated mice, or the relative tissue distribution to liver and small intestinal tissue compared to single elacridar-treated mice. Importantly, no signs of toxicity were observed in this experiment, suggesting that double boosting with elacridar and ritonavir does not uncover unexpected toxicities of this ALK inhibitor, at least in mice, which contrasts with what we have observed with some other ALK inhibitor drugs [31].

3.3. Oral bioavailability of lorlatinib

To date, very little information is publicly available on the oral bioavailability of lorlatinib, a macrocyclic ALK inhibitor with high hydrophobicity and membrane permeability properties. To assess the possible impact of mouse Cyp3a or human CYP3A4 on lorlatinib oral availability, wild-type, *Cyp3a*$^{-/-}$, and Cyp3aXAV mice received lorlatinib either orally or intravenously, at dosages of 10 mg/kg and 5 mg/kg, respectively. In the intravenous administration group, no significant differences were observed in the lorlatinib plasma AUC_{0-8h} in *Cyp3a*$^{-/-}$ and Cyp3aXAV mice compared to wild-type mice (Fig. 5A; Table 3). However, the lorlatinib systemic exposure was 1.3-fold higher (Table 3; $P < 0.05$) in *Cyp3a*$^{-/-}$ mice compared to humanized Cyp3aXAV mice. These data suggest that human CYP3A4 has some impact on lorlatinib metabolism, inducing somewhat lower plasma exposure of lorlatinib upon intravenous administration.

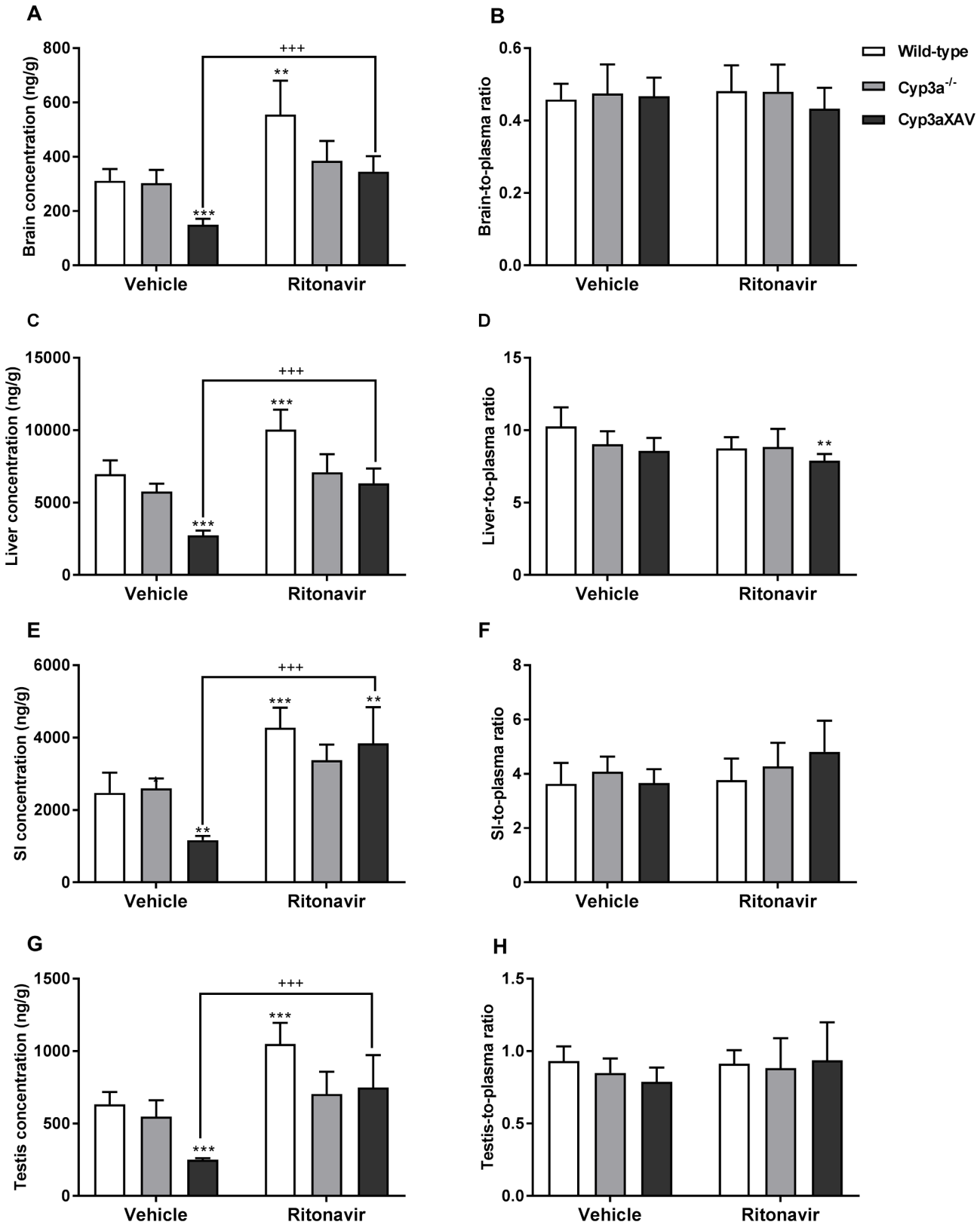

Fig. 2. Tissue distribution of lorlatinib in male wild-type, *Cyp3a*$^{-/-}$ and Cyp3aXAV mice 8 h after oral administration of 10 mg/kg lorlatinib. Vehicle or 25 mg/kg ritonavir was orally administered 15 min prior to lorlatinib administration. Panels reflect brain, liver, small intestinal tissue (SI), or testis concentrations (Panel A, C, E, or D) and organ-to-plasma ratios (Panel B, D, F, or H). *, $P < 0.05$; **, $P < 0.01$; ***, $P < 0.001$ compared to vehicle-treated wild-type mice; $^{+}$, $P < 0.05$; $^{++}$, $P < 0.01$; $^{+++}$, $P < 0.001$ comparing Cyp3aXAV mice with or without ritonavir. Data are presented as mean ± S.D. (n = 5–7).

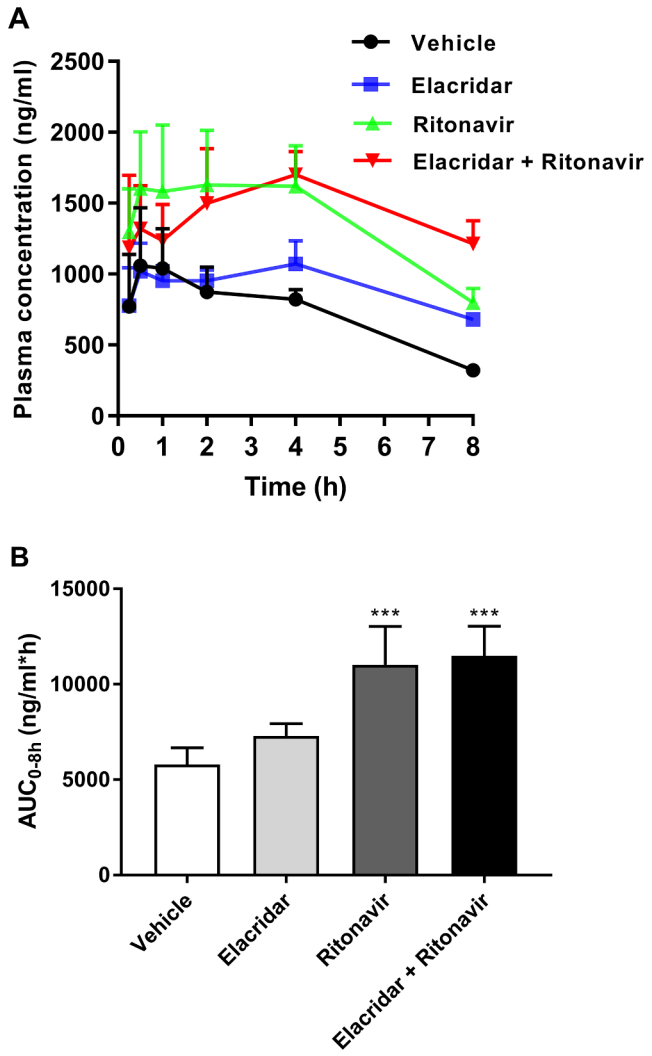

Fig. 3. Plasma concentration-time curves and plasma $AUC_{0\text{-}8h}$ of lorlatinib over 8 h after oral administration of 10 mg/kg lorlatinib to male Cyp3aXAV mice with vehicle, elacridar (100 mg/kg), ritonavir (25 mg/kg), or combined elacridar (100 mg/kg) and ritonavir (25 mg/kg) coadministration (n = 5–7). Vehicle or boosters were orally administered 15 min prior to lorlatinib administration. Panel A: plasma concentration-time curves of lorlatinib. Panel B: plasma $AUC_{0\text{-}8h}$ of lorlatinib. *, $P < 0.05$; **, $P < 0.01$; ***, $P < 0.001$ compared to vehicle-treated Cyp3aXAV mice.

In the oral administration group, we did observe a clear, 1.6-fold ($P < 0.001$) lower oral plasma $AUC_{0\text{-}8h}$ in Cyp3aXAV mice compared to wild-type and *Cyp3a*$^{-/-}$ mice (Fig. 5B; Table 3), whereas wild-type and *Cyp3a*$^{-/-}$ mice displayed similar plasma exposure levels. These data are in line with the results of our preceding ritonavir experiment (Fig. 1). The relative tissue distribution of lorlatinib at 8 h was not at all affected by oral or intravenous administration, or in any of the mouse strains, as illustrated by virtually equal tissue-to-plasma ratios in all the tested mouse strains (Supplemental Fig. 2).

The absolute oral bioavailability values of lorlatinib calculated from the i.v. and oral plasma exposure data over 8 h in wild-type, *Cyp3a*$^{-/-}$, and Cyp3aXAV mice were 81.6%, 72.9%, and 58.5%, respectively (Fig. 6; Table 3). This indicates that lorlatinib has good oral bioavailability, as would be expected based on its highly hydrophobic and membrane permeability properties. There was no significant difference between wild-type and *Cyp3a*$^{-/-}$ mice, indicating again that mouse Cyp3a has little impact on restricting oral availability of lorlatinib. However, the oral bioavailability of lorlatinib in Cyp3aXAV mice was significantly lower than that in wild-type mice ($P < 0.05$), but not than that in *Cyp3a*$^{-/-}$ mice ($P = 0.126$). Since mouse Cyp3a does not limit the oral bioavailability, the impact of human CYP3A4 on restricting bioavailability was clear based on our data. Qualitatively similar results were obtained when using the $AUC_{0\text{-}inf}$ for these three mouse strains. This supports our previous demonstration that human CYP3A4 plays an important role in limiting plasma exposure of lorlatinib. Lorlatinib thus has a relatively good oral bioavailability, which could be significantly restricted by human CYP3A4, but not by mouse Cyp3a.

OATP-mediated liver uptake can also affect the oral bioavailability of drugs [32,33]. Very little is known about possible lorlatinib interactions with OATP/SLCO uptake transporters. We therefore performed a pilot experiment administering oral lorlatinib (10 mg/kg) to wild-type and Oatp1a/1b-deficient mice, and analyzed plasma concentrations up till 8 h and the liver-to-plasma ratio at 8 h. The results were not significantly different between wild-type and Oatp1a/1b-deficient mice (data not shown), suggesting that there is no meaningful impact of mouse Oatp1a/1b transporters on lorlatinib oral availability. This project line was therefore not further pursued.

4. Discussion

We demonstrate here that the lorlatinib plasma $AUC_{0\text{-}8h}$ in CYP3A4-humanized mice could be increased 1.9-fold by oral coadministration of the CYP3A inhibitor ritonavir, reverting to levels seen in *Cyp3a*$^{-/-}$ (and wild-type) mice, without altering the relative tissue distribution of lorlatinib (Figs. 1 and 2; Table 1). Furthermore, simultaneous pharmacological inhibition of both P-gp and CYP3A4 by coadministration of elacridar and ritonavir together to CYP3A4-humanized mice increased the absolute brain concentrations of lorlatinib at 8 h by 16-fold, and the relative brain concentration by 4-fold, whereas the plasma $AUC_{0\text{-}8h}$ was 2-fold increased (Figs. 3 and 4; Table 2). The relative tissue distribution to most other organs was not affected by ritonavir and/or elacridar coadministration, except for testis, which qualitatively followed the brain behavior. The oral bioavailability of lorlatinib was quite high (55.8–81.6%), but still significantly restricted by human CYP3A4 activity (Fig. 6; Table 3). We further found that the multispecific Oatp1a/1b drug uptake transporters had no significant impact on the oral availability or liver distribution of lorlatinib.

Oral administration of ritonavir, a highly potent CYP3A inhibitor, caused a 1.9-fold increase in plasma AUC of oral lorlatinib in CYP3A4-humanized mice, but had no marked impact in wild-type and *Cyp3a*$^{-/-}$ mice. This suggests that mouse Cyp3a, in contrast to human CYP3A4, plays little or no role in limiting the oral availability of lorlatinib. It also suggests that no other lorlatinib-metabolizing enzymes were affected by ritonavir. Given our demonstration that pharmacological inhibition of human CYP3A4 could substantially alter the pharmacokinetics of lorlatinib, this might also affect the therapeutic efficacy and toxicity of lorlatinib in human patients. Deliberate or coincidental coadministration of CYP3A-inhibiting drugs may increase the effective exposure of lorlatinib in patients. Conversely, CYP3A inducers, such as rifampicin [34] and carbamazepine [35], can increase the activity of CYP3A4, thus resulting in lower plasma exposure of lorlatinib in patients. Of note, the relative tissue distribution of lorlatinib was not substantially affected by ritonavir. This suggests that ritonavir coadministration may be a way to boost systemic exposure of oral lorlatinib in patients without invoking the risk of altering tissue distribution, which might result in altered toxicity or other side effects of this drug. In fact, given the usually high cost of novel anticancer drugs, one could even consider to deliberately co-administer lorlatinib with ritonavir in order to reduce the dose of lorlatinib necessary to achieve therapeutic plasma levels of the drug in patients. For instance, halving the dose and therefore cost of lorlatinib therapy might already yield substantial savings in health care costs.

Table 2
Plasma, brain and testis pharmacokinetic parameters of lorlatinib over 8 h after oral administration of 10 mg/kg lorlatinib to male Cyp3aXAV mice with vehicle, elacridar, ritonavir, or combined elacridar and ritonavir coadministration.

Parameter	Type of pre-treatment			
	Vehicle	Elacridar	Ritonavir	Elacridar and Ritonavir
$AUC_{0\text{-}8h}$, ng/ml h	5792 ± 871	7295 ± 633	11013 ± 2023***	11500 ± 1548***
Fold increase $AUC_{0\text{–}8h}$	1.00	1.26	1.90	1.99
C_{max}, ng/ml	1145 ± 327	1155 ± 129	1766 ± 345	1759 ± 221
T_{max}, h	0.5–4.0	0.5–4.0	0.5–4.0	0.25–4.0
C_{brain}, ng/g	150 ± 22	1211 ± 97***	345 ± 57	2466 ± 302$^{***(\#\#\#)}$
Fold increase C_{brain}	1.00	8.07	2.30	16.44
Brain-to-plasma ratio	0.47 ± 0.05	1.78 ± 0.08***	0.43 ± 0.06	2.04 ± 0.15$^{***(\#\#)}$
Fold change ratio	1.00	3.79	0.91	4.34
C_{testis}, ng/g	250 ± 11	1101 ± 96*	750 ± 223	2337 ± 712$^{***(\#\#\#)}$
Fold increase C_{testis}	1.00	4.40	3.00	9.35
Testis-to-plasma ratio	0.79 ± 0.10	1.63 ± 0.16***	0.94 ± 0.26	1.90 ± 0.30***
Fold increase ratio	1.00	2.06	1.19	2.41

Data are presented as mean ± S.D. (n = 5–7). Lorlatinib was administered alone or orally coadministered with 100 mg/kg elacridar, 25 mg/kg ritonavir, or 100 mg/kg elacridar and 25 mg/kg ritonavir combined 15 min before lorlatinib administration. $AUC_{0\text{-}8h}$, area under plasma concentration-time curve; C_{max}, maximum concentration in plasma; T_{max}, time point (h) of maximum plasma concentration (range for individual mice); $C_{brain/testis}$, brain/testis concentration; $P_{brain/testis}$, brain/testis accumulation. *, $P < 0.05$; **, $P < 0.01$; ***, $P < 0.001$ compared to vehicle-treated Cyp3aXAV mice; $^{\#}$, $P < 0.05$; $^{\#\#}$, $P < 0.01$; $^{\#\#\#}$, $P < 0.001$ comparing Cyp3aXAV mice with coadministration of both elacridar and ritonavir to Cyp3aXAV mice with coadministration of only elacridar.

In our preceding study, we found that the oral plasma $AUC_{0\text{-}8h}$ of lorlatinib was slightly but significantly higher (1.3-fold) in female *Cyp3a*$^{-/-}$ mice compared to wild-type mice [20]. However, in the current study with male mice we did not observe a significant increase in lorlatinib plasma exposure due to either knockout or targeted inhibition of mouse Cyp3a. The difference in mouse gender is the most probable cause of this modest difference. It may be that in mice lorlatinib is primarily metabolized or eliminated by some other enzymes than Cyp3a.

Utilizing drug-structure based design, lorlatinib was developed as a macrocyclic ALK inhibitor with high lipophilicity and good CNS penetration [15,20]. Lorlatinib was reported to be only slightly transported by ABCB1 *in vitro*, as demonstrated in an ABCB1-overexpressing MDCK cell line (active efflux ratio $r = 1.5$) [15]. Moreover, P-gp overexpression in ceritinib-resistant patient-derived cells did not confer lorlatinib resistance [36]. However, we previously showed that genetic knockout or pharmacological inhibition with elacridar of ABCB1 could still substantially boost lorlatinib penetration into the brain in wild-type mice [20]. This clearly demonstrated that P-gp can still play an important role in limiting lorlatinib brain distribution, at least in mice. Some patients can show progression of brain metastases after an initial positive response to lorlatinib [37]. Although speculative at this time, one could consider the possibility that there might be a physiological "adaptation" at or around the tumor, with up-regulated expression of ABCB1 at the BBB or in the tumor cells themselves, resulting in limited therapeutic efficacy due to reduced local concentrations of lorlatinib.

In the present study, we used CYP3A4-humanized mice to mimic a patient situation in order to investigate to what extent the pharmacokinetics of lorlatinib can be altered by simultaneous chemical inhibition of both P-gp and CYP3A4 using elacridar and ritonavir. We found here that upon treatment with combined elacridar and ritonavir absolute brain concentrations of lorlatinib were increased by 16-fold compared to untreated mice, and by 2-fold compared to single-elacridar treated mice. Adding ritonavir to the treatment left the brain-to-plasma ratios not much changed, indicating that the increased brain concentrations due to ritonavir were primarily a consequence of the increased plasma concentrations. Also liver, small intestinal tissue, and testis showed qualitatively similar results of the added ritonavir, reflecting the increase in plasma concentrations. Furthermore, the brain-to-plasma ratios in both elacridar-treated groups (with or without ritonavir) were compatible with those we observed previously in *Abcb1a/1b;Abcg2*$^{-/-}$ mice [20], suggesting complete inhibition of ABCB1 and ABCG2 in the BBB, resulting in highly increased brain concentrations of lorlatinib. Moreover, addition of elacridar to the ritonavir treatment did not further increase the plasma exposure of lorlatinib. These data thus suggest a relatively specific action of each of the booster drugs. In case it would turn out that it is desirable to increase the brain penetration of lorlatinib, especially for NSCLC patients with brain metastases, elacridar would likely allow this without inducing additional systemic toxicity due to higher plasma exposure.

Our data suggest a clear impact of drug-drug interactions on the pharmacokinetics of lorlatinib. However, unlike the 7-fold increase in plasma exposure of docetaxel observed upon oral ritonavir coadministration [26], ritonavir only boosted the oral availability of lorlatinib by 2-fold. Moreover, elacridar also did not show as strong an impact on increasing the brain penetration of lorlatinib (4-fold) as for the first-generation ALK inhibitor crizotinib (12-fold) [38]. These comparatively modest interactions between the P-gp and CYP3A4 inhibitors and lorlatinib also reduce the chance of dramatic changes in possible toxicity of lorlatinib. However, variation in P-gp and CYP3A4 activity, in view of this clear drug-drug interaction, should still be an element that will need to be considered in the clinical dosing of lorlatinib.

It is worth noting that we did not observe any signs of toxicity of lorlatinib in any of the mouse strains that we tested with oral lorlatinib at 10 mg/kg or intravenous lorlatinib at 5 mg/kg, either in the absence or in the presence of boosters. This suggests that lorlatinib may have a better safety profile than some other ALK inhibitors. We recently found that brigatinib, a second-generation ALK inhibitor, showed severe, and sometimes even lethal toxicity in *Abcb1a/1b*$^{-/-}$ and *Abcb1a/1b;Abcg2*$^{-/-}$ mice, or in wild-type mice treated with lower doses of brigatinib (5 mg/kg) and elacridar (50 mg/kg) [31]. Although no signs of toxicity were observed in mice in the present lorlatinib study, modest cognitive toxicity emerged in lorlatinib-treated patients [19], potentially related to a relatively high capacity of lorlatinib to cross the BBB. Therefore, potential toxicity and dose adjustment should first be very carefully monitored in patients when they receive lorlatinib coadministered with P-gp and/or CYP3A4 inhibitors in order to optimize its pharmacokinetic behavior.

Oral administration is usually the preferred administration route in terms of its convenience in administration, cost, ease of design, the option to use a variety of formulations, and most importantly, better patient compliance especially for chronic treatments [39]. However, many anticancer drugs are limited due to first-pass effect [40], poor solubility [41], low intrinsic permeability of drug barriers,

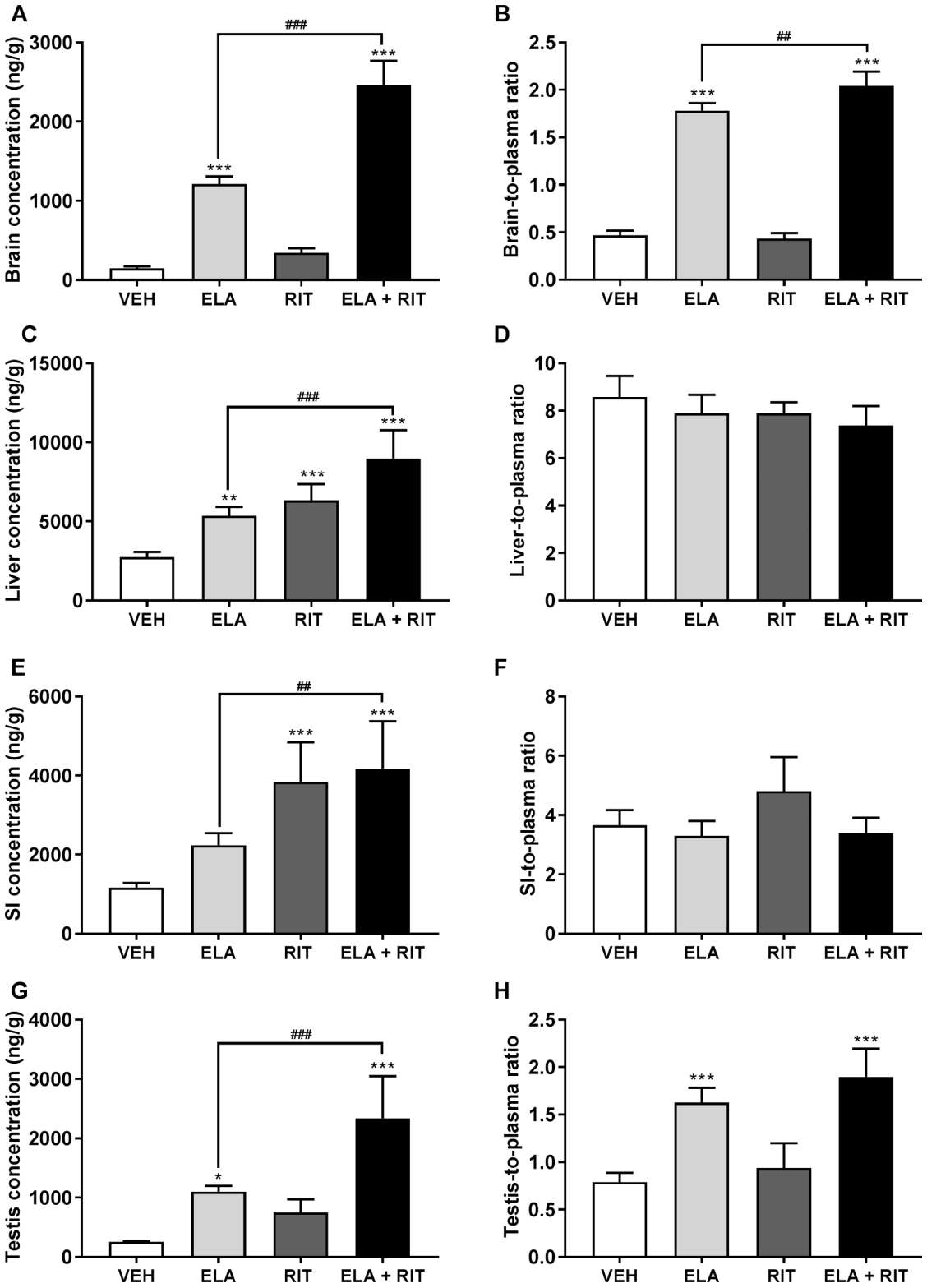

Fig. 4. Tissue distribution of lorlatinib in male Cyp3aXAV mice 8 h after oral administration of 10 mg/kg lorlatinib with vehicle, elacridar (100 mg/kg), ritonavir (25 mg/kg), or combined elacridar (100 mg/kg) and ritonavir (25 mg/kg) coadministration. Panels reflect brain, liver, small intestinal tissue (SI), or testis concentrations (Panel A, C, E, or D) and organ-to-plasma ratios (Panel B, D, F, or H). Vehicle or booster(s) were orally administered 15 min prior to lorlatinib administration. *, $P < 0.05$; **, $P < 0.01$; ***, $P < 0.001$ compared to vehicle-treated Cyp3aXAV mice; $^{\#}$, $P < 0.05$; $^{\#\#}$, $P < 0.01$; $^{\#\#\#}$, $P < 0.001$ comparing Cyp3aXAV mice with coadministration of elacridar to those with combined coadministration of elacridar and ritonavir. Data are presented as mean ± S.D. (n = 5–7). (VEH: vehicle; ELA: elacridar; RIT: ritonavir).

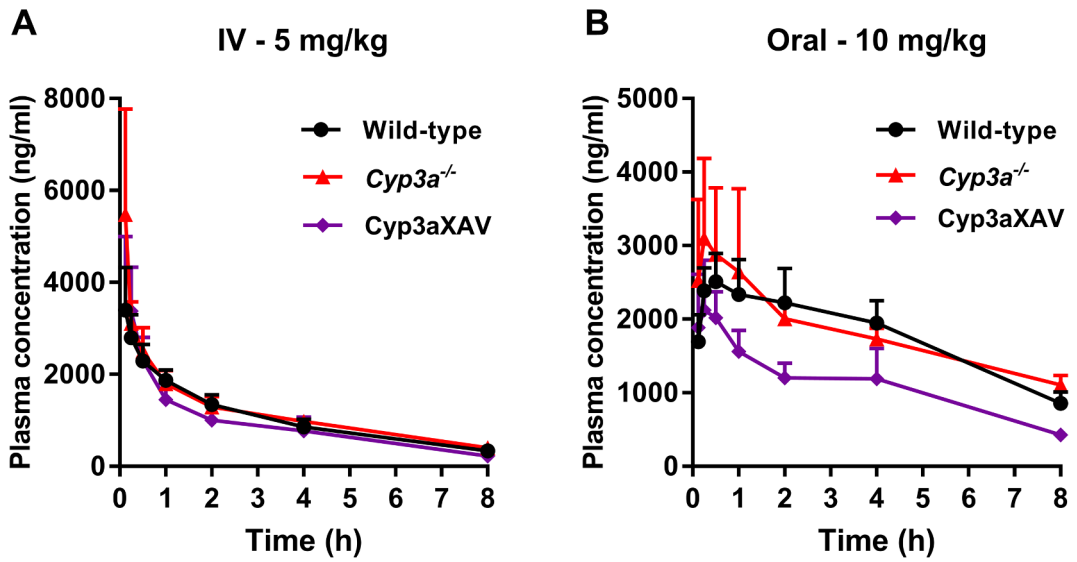

Fig. 5. Plasma concentration-time curves of lorlatinib in male wild-type, *Cyp3a*$^{-/-}$, and Cyp3aXAV mice over 8 h after intravenous injection (Panel A) or oral administration (Panel B) of 5 mg/kg or 10 mg/kg lorlatinib, respectively. Data are presented as mean ± S.D. (n = 5–8).

bioavailability and so on [42]. Lorlatinib is recommended to be administered orally in the clinic. We found that lorlatinib has good oral bioavailability, although it could be modestly but significantly restricted by human CYP3A4, but not by mouse Cyp3a. This high bioavailability is in line with what would be expected based on the biophysical properties of lorlatinib, and likely supports limited inter- and intra-patient variation in availability of this drug. Overall, it therefore appears that lorlatinib shows a number of positive pharmacokinetic characteristics that validate the effort that was put into designing this drug as a highly membrane-permeable compound [15]. The absence of a noticeable impact of Oatp1a/1b transporters on lorlatinib pharmacokinetics may also relate to these properties.

In summary, we demonstrated drug-drug interactions between lorlatinib and inhibitors of P-gp and CYP3A4. Ritonavir could markedly enhance the systemic exposure without altering the relative tissue distribution of lorlatinib. Coadministration of combined elacridar and ritonavir could further markedly increase the absolute brain concentrations of lorlatinib. Furthermore, we found that lorlatinib has a quite high oral bioavailability. While the findings in this study will obviously need to be tested in their own right for their validity in patients, we expect that they will help to optimize the clinical application of lorlatinib.

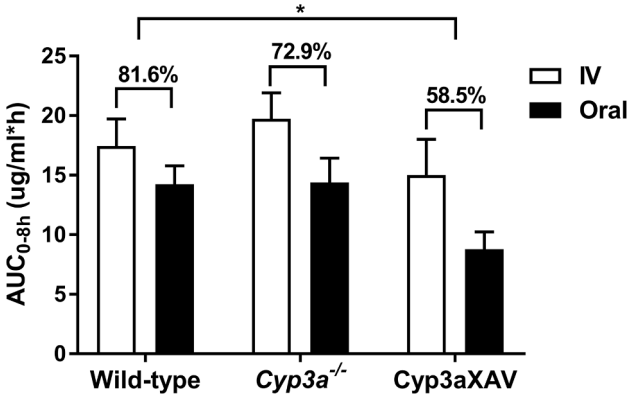

Fig. 6. Oral and intravenous (IV) plasma AUC and oral bioavailability of lorlatinib in male wild-type, *Cyp3a*$^{-/-}$, and Cyp3aXAV mice over 8 h. Percentage values indicate AUC_{Oral}/AUC_{IV} for each strain. The dose-normalized oral and i.v. plasma AUC_{0-8h} was used. Data are presented as mean ± S.D. (n = 5–8). *, $P < 0.05$ comparing oral bioavailability to that in wild-type mice.

Table 3
Plasma pharmacokinetic parameters over 8 h after intravenous (5 mg/kg) or oral (10 mg/kg) administration of lorlatinib to male wild-type, *Cyp3a*$^{-/-}$ and Cyp3aXAV mice.

Treatment	Parameter	Genotype		
		Wild-type	*Cyp3a*$^{-/-}$	Cyp3aXAV
Intravenous injection (5 mg/kg)	AUC_{0-8h}, ng/ml h	8726 ± 1137	9865 ± 1091	7510 ± 1493$^{(\#)}$
	Fold change AUC_{0-8h}	1.00	1.13	0.86
	$T_{1/2}$, h	3.0 ± 0.3	3.4 ± 0.4	2.6 ± 0.5$^{(\#)}$
Oral administration (10 mg/kg)	AUC_{0-8h}, ng/ml h	14242 ± 1540	14377 ± 2050	8788 ± 1446$^{***(\#\#\#)}$
	Fold change AUC_{0-8h}	1.00	1.01	0.62
	C_{max}, ng/ml	2679 ± 308	3193 ± 952	2406 ± 613
	T_{max}, h	0.25–4	0.25–2	0.125–0.5
	Oral bioavailability (%)	81.6	72.9	58.5*

Data are presented as mean ± S.D. (n = 5–8). AUC_{0-8h}, area under plasma concentration-time curve; $T_{1/2}$, elimination half-life; C_{max}, maximum concentration in plasma; T_{max} , time point (h) of maximum plasma concentration (range for individual mice). *, $P < 0.05$; **, $P < 0.01$; ***, $P < 0.001$ compared to wild-type mice. $^{\#}$, $P < 0.05$; $^{\#\#}$, $P < 0.01$; $^{\#\#\#}$, $P < 0.001$ comparing Cyp3aXAV to *Cyp3a*$^{-/-}$ mice.

Conflict of interest

The research group of Alfred H. Schinkel receives revenue from commercial distribution of some of the mouse strains used in this study. The remaining authors declare no conflict of interest.

Acknowledgement

This work was funded in part by the China Scholarship Council (CSC Scholarship No. 201606220081).

Appendix A. Supplementary material

Supplementary data to this article can be found online at https://doi.org/10.1016/j.ejpb.2019.01.016.

References

[1] R.L. Siegel, K.D. Miller, A. Jemal, Cancer statistics, 2018, CA: A Cancer Journal for Clinicians, 2018.
[2] D.S. Ettinger, W. Akerley, G. Bepler, M.G. Blum, A. Chang, R.T. Cheney, L.R. Chirieac, T.A. D'Amico, T.L. Demmy, A.K. Ganti, R. Govindan, F.W. Grannis Jr., T. Jahan, M. Jahanzeb, D.H. Johnson, A. Kessinger, R. Komaki, F.M. Kong, M.G. Kris, L.M. Krug, Q.T. Le, I.T. Lennes, R. Martins, J. O'Malley, R.U. Osarogiagbon, G.A. Otterson, J.D. Patel, K.M. Pisters, K. Reckamp, G.J. Riely, E. Rohren, G.R. Simon, S.J. Swanson, D.E. Wood, S.C. Yang, Non-small cell lung cancer, J. Natl. Compr. Can. Network: JNCCN 8 (2010) 740–801.
[3] E. Grande, M.V. Bolos, E. Arriola, Targeting oncogenic ALK: a promising strategy for cancer treatment, Mol. Cancer Ther. 10 (2011) 569–579.
[4] E.L. Kwak, Y.J. Bang, D.R. Camidge, A.T. Shaw, B. Solomon, R.G. Maki, S.H. Ou, B.J. Dezube, P.A. Janne, D.B. Costa, M. Varella-Garcia, W.H. Kim, T.J. Lynch, P. Fidias, H. Stubbs, J.A. Engelman, L.V. Sequist, W. Tan, L. Gandhi, M. Mino-Kenudson, G.C. Wei, S.M. Shreeve, M.J. Ratain, J. Settleman, J.G. Christensen, D.A. Haber, K. Wilner, R. Salgia, G.I. Shapiro, J.W. Clark, A.J. Iafrate, Anaplastic lymphoma kinase inhibition in non-small-cell lung cancer, New England J. Med. 363 (2010) 1693–1703.
[5] D.B. Costa, A.T. Shaw, S.H. Ou, B.J. Solomon, G.J. Riely, M.J. Ahn, C. Zhou, S.M. Shreeve, P. Selaru, A. Polli, P. Schnell, K.D. Wilner, R. Wiltshire, D.R. Camidge, L. Crino, Clinical experience with crizotinib in patients with advanced ALK-rearranged non-small-cell lung cancer and brain metastases, J. Clin. Oncol.: Off. J. Am. Soc. Clin. Oncol. 33 (2015) 1881–1888.
[6] A.T. Shaw, L. Gandhi, S. Gadgeel, G.J. Riely, J. Cetnar, H. West, D.R. Camidge, M.A. Socinski, A. Chiappori, T. Mekhail, B.H. Chao, H. Borghaei, K.A. Gold, A. Zeaiter, W. Bordogna, B. Balas, O. Puig, V. Henschel, S.I. Ou, Alectinib in ALK-positive, crizotinib-resistant, non-small-cell lung cancer: a single-group, multicentre, phase 2 trial, Lancet. Oncol. 17 (2016) 234–242.
[7] L. Friboulet, N. Li, R. Katayama, C.C. Lee, J.F. Gainor, A.S. Crystal, P.Y. Michellys, M.M. Awad, N. Yanagitani, S. Kim, A.C. Pferdekamper, J. Li, S. Kasibhatla, F. Sun, X. Sun, S. Hua, P. McNamara, S. Mahmood, E.L. Lockerman, N. Fujita, M. Nishio, J.L. Harris, A.T. Shaw, J.A. Engelman, The ALK inhibitor ceritinib overcomes crizotinib resistance in non-small cell lung cancer, Can. Discov. 4 (2014) 662–673.
[8] D.R. Camidge, H.R. Kim, M.J. Ahn, J.C. Yang, J.Y. Han, J.S. Lee, M.J. Hochmair, J.Y. Li, G.C. Chang, K.H. Lee, C. Gridelli, A. Delmonte, R. Garcia Campelo, D.W. Kim, A. Bearz, F. Griesinger, A. Morabito, E. Felip, R. Califano, S. Ghosh, A. Spira, S.N. Gettinger, M. Tiseo, N. Gupta, J. Haney, D. Kerstein, S. Popat, Brigatinib versus Crizotinib in ALK-positive non-small-cell lung cancer, New Engl. J. Med. 379 (2018) 2027–2039.
[9] A.S. Crystal, A.T. Shaw, L.V. Sequist, L. Friboulet, M.J. Niederst, E.L. Lockerman, R.L. Frias, J.F. Gainor, A. Amzallag, P. Greninger, D. Lee, A. Kalsy, M. Gomez-Caraballo, L. Elamine, E. Howe, W. Hur, E. Lifshits, H.E. Robinson, R. Katayama, A.C. Faber, M.M. Awad, S. Ramaswamy, M. Mino-Kenudson, A.J. Iafrate, C.H. Benes, J.A. Engelman, Patient-derived models of acquired resistance can identify effective drug combinations for cancer (New York, N.Y.), Science 346 (2014) 1480–1486.
[10] R. Katayama, A.T. Shaw, T.M. Khan, M. Mino-Kenudson, B.J. Solomon, B. Halmos, N.A. Jessop, J.C. Wain, A.T. Yeo, C. Benes, L. Drew, J.C. Saeh, K. Crosby, L.V. Sequist, A.J. Iafrate, J.A. Engelman, Mechanisms of acquired crizotinib resistance in ALK-rearranged lung Cancers, Sci. Transl. Med. 4 (2012) 120ra117.
[11] C.M. Lovly, N.T. McDonald, H. Chen, S. Ortiz-Cuaran, L.C. Heukamp, Y. Yan, A. Florin, L. Ozretic, D. Lim, L. Wang, Z. Chen, X. Chen, P. Lu, P.K. Paik, R. Shen, H. Jin, R. Buettner, S. Ansen, S. Perner, M. Brockmann, M. Bos, J. Wolf, M. Gardizi, G.M. Wright, B. Solomon, P.A. Russell, T.M. Rogers, Y. Suehara, M. Red-Brewer, R. Tieu, E. de Stanchina, Q. Wang, Z. Zhao, D.H. Johnson, L. Horn, K.K. Wong, R.K. Thomas, M. Ladanyi, W. Pao, Rationale for co-targeting IGF-1R and ALK in ALK fusion-positive lung cancer, Nat. Med. 20 (2014) 1027–1034.
[12] D. Maillet, I. Martel-Lafay, D. Arpin, M. Perol, Ineffectiveness of crizotinib on brain metastases in two cases of lung adenocarcinoma with EML4-ALK rearrangement, J. Thor. Oncol.: Off. Publ. Int. Assoc. Study of Lung Can. 8 (2013) e30–e31.
[13] G. Toyokawa, T. Seto, Updated evidence on the mechanisms of resistance to ALK inhibitors and strategies to overcome such resistance: clinical and preclinical data, Oncol. Res. Treat. 38 (2015) 291–298.
[14] S. Gadgeel, S. Peters, T. Mok, A.T. Shaw, D.W. Kim, S.I. Ou, M. Perol, A. Wrona, S. Novello, R. Rosell, A. Zeaiter, T. Liu, E. Nuesch, B. Balas, D.R. Camidge, Alectinib versus crizotinib in treatment-naive anaplastic lymphoma kinase-positive (ALK+) non-small-cell lung cancer: CNS efficacy results from the ALEX study, Ann. Oncol.: Off. J. Eur. Soc. Med. Oncol. 29 (2018) 2214–2222.
[15] T.W. Johnson, P.F. Richardson, S. Bailey, A. Brooun, B.J. Burke, M.R. Collins, J.J. Cui, J.G. Deal, Y.L. Deng, D. Dinh, L.D. Engstrom, M. He, J. Hoffman, R.L. Hoffman, Q. Huang, R.S. Kania, J.C. Kath, H. Lam, J.L. Lam, P.T. Le, L. Lingardo, W. Liu, M. McTigue, C.L. Palmer, N.W. Sach, T. Smeal, G.L. Smith, A.E. Stewart, S. Timofeevski, H. Zhu, J. Zhu, H.Y. Zou, M.P. Edwards, Discovery of (10R)-7-amino-12-fluoro-2,10,16-trimethyl-15-oxo-10,15,16,17-tetrahydro-2H-8,4-(m etheno)pyrazolo[4,3-h][2,5,11]-benzoxadiazacyclotetradecine-3-carbonitrile (PF-06463922), a macrocyclic inhibitor of anaplastic lymphoma kinase (ALK) and c-ros oncogene 1 (ROS1) with preclinical brain exposure and broad-spectrum potency against ALK-resistant mutations, J. Med. Chem. 57 (2014) 4720–4744.
[16] H.Y. Zou, L. Friboulet, D.P. Kodack, L.D. Engstrom, Q. Li, M. West, R.W. Tang, H. Wang, K. Tsaparikos, J. Wang, S. Timofeevski, R. Katayama, D.M. Dinh, H. Lam, J.L. Lam, S. Yamazaki, W. Hu, B. Patel, D. Bezwada, R.L. Frias, E. Lifshits, S. Mahmood, J.F. Gainor, T. Affolter, P.B. Lappin, H. Gukasyan, N. Lee, S. Deng, R.K. Jain, T.W. Johnson, A.T. Shaw, V.R. Fantin, T. Smeal, PF-06463922, an ALK/ROS1, inhibitor overcomes resistance to first and second generation ALK inhibitors in preclinical models, Can. cell 28 (2015) 70–81.
[17] A.T. Shaw, T.M. Bauer, E. Felip, B. Besse, L.P. James, J.S. Clancy, G. Mugundu, J.-F. Martini, A. Abbattista, B.J. Solomon, Clinical activity and safety of PF-06463922 from a dose escalation study in patients with advanced ALK+ or ROS1+ NSCLC, J. Clin. Oncol. 33 (2015) 8018-8018.
[18] A.T. Shaw, E. Felip, T.M. Bauer, B. Besse, A. Navarro, S. Postel-Vinay, J.F. Gainor, M. Johnson, J. Dietrich, L.P. James, J.S. Clancy, J. Chen, J.-F. Martini, A. Abbattista, B.J. Solomon, Lorlatinib in non-small-cell lung cancer with ALK or ROS1 rearrangement: an international, multicentre, open-label, single-arm first-in-man phase 1 trial, Lancet. Oncol. 18 (2017) 1590–1599.
[19] B.J. Solomon, B. Besse, T.M. Bauer, E. Felip, R.A. Soo, D.R. Camidge, R. Chiari, A. Bearz, C.C. Lin, S.M. Gadgeel, G.J. Riely, E.H. Tan, T. Seto, L.P. James, J.S. Clancy, A. Abbattista, J.F. Martini, J. Chen, G. Peltz, H. Thurm, S.H. Ignatius Ou, A.T. Shaw, Lorlatinib in patients with ALK-positive non-small-cell lung cancer: results from a global phase 2 study, Lancet Oncol. 19 (2018) 1654–1667.
[20] W. Li, R.W. Sparidans, Y. Wang, M.C. Lebre, E. Wagenaar, J.H. Beijnen, A.H. Schinkel, P-glycoprotein (MDR1/ABCB1) restricts brain accumulation and cytochrome P450–3A (CYP3A) limits oral availability of the novel ALK/ROS1 inhibitor lorlatinib, Int. J. Can. 143 (2018) 2029–2038.
[21] P. Borst, R.O. Elferink, Mammalian ABC transporters in health and disease, Annu. Rev. Biochem. 71 (2002) 537–592.
[22] A.H. Schinkel, J.W. Jonker, Mammalian drug efflux transporters of the ATP binding cassette (ABC) family: an overview, Adv. Drug Deliv. Rev. 55 (2003) 3–29.
[23] K. Thelen, J.B. Dressman, Cytochrome P450-mediated metabolism in the human gut wall, J. Pharm. Pharmacol. 61 (2009) 541–558.
[24] M.F. Paine, H.L. Hart, S.S. Ludington, R.L. Haining, A.E. Rettie, D.C. Zeldin, The human intestinal cytochrome P450 "pie", Drug Metabol. Disposit.: Biol. Fate Chem. 34 (2006) 880–886.
[25] R.A. van Waterschoot, R. ter Heine, E. Wagenaar, C.M. van der Kruijssen, R.W. Rooswinkel, A.D. Huitema, J.H. Beijnen, A.H. Schinkel, Effects of cytochrome P450 3A (CYP3A) and the drug transporters P-glycoprotein (MDR1/ABCB1) and MRP2 (ABCC2) on the pharmacokinetics of lopinavir, Br. J. Pharmacol. 160 (2010) 1224–1233.
[26] J.J. Hendrikx, J.S. Lagas, J.Y. Song, H. Rosing, J.H. Schellens, J.H. Beijnen, S. Rottenberg, A.H. Schinkel, Ritonavir inhibits intratumoral docetaxel metabolism and enhances docetaxel antitumor activity in an immunocompetent mouse breast cancer model, Int. J. Cancer 138 (2016) 758–769.
[27] C. Spatari, W. Li, A.H. Schinkel, G. Ragno, J.H.M. Schellens, J.H. Beijnen, R.W. Sparidans, Bioanalytical assay for the quantification of the ALK inhibitor lorlatinib in mouse plasma using liquid chromatography-tandem mass spectrometry, J. Chromatogr. B, Anal. Technol. Biomed. Life Sci. 1083 (2018) 204–208.
[28] R.W. Sparidans, W. Li, A.H. Schinkel, J.H.M. Schellens, J.H. Beijnen, Bioanalytical liquid chromatography-tandem mass spectrometric assay for the quantification of the ALK inhibitors alectinib, brigatinib and lorlatinib in plasma and mouse tissue homogenates, J. Pharm. Biomed. Anal. 161 (2018) 136–143.
[29] A.E. van Herwaarden, E. Wagenaar, C.M. van der Kruijssen, R.A. van Waterschoot, J.W. Smit, J.Y. Song, M.A. van der Valk, O. van Tellingen, J.W. van der Hoorn, H. Rosing, J.H. Beijnen, A.H. Schinkel, Knockout of cytochrome P450 3A yields new mouse models for understanding xenobiotic metabolism, J. Clin. Investig. 117 (2007) 3583–3592.
[30] D.T. Holmes, K.A. Buhr, Error propagation in calculated ratios, Clin. Biochem. 40 (2007) 728–734.
[31] W. Li, R.W. Sparidans, Y. Wang, M.C. Lebre, J.H. Beijnen, A.H. Schinkel, P-glycoprotein and breast cancer resistance protein restrict brigatinib brain accumulation and toxicity, and alongside CYP3A, limit its oral availability, Pharmacol. Res. 137 (2018) 47–55.
[32] D. Iusuf, A. van Esch, M. Hobbs, M. Taylor, K.E. Kenworthy, E. van de Steeg, E. Wagenaar, A.H. Schinkel, Murine Oatp1a/1b uptake transporters control rosuvastatin systemic exposure without affecting its apparent liver exposure, Mol. Pharmacol. 83 (2013) 919–929.
[33] E. van de Steeg, E. Wagenaar, C.M. van der Kruijssen, J.E. Burggraaff, D.R. de Waart, R.P. Elferink, K.E. Kenworthy, A.H. Schinkel, Organic anion transporting polypeptide 1a/1b-knockout mice provide insights into hepatic handling of bilirubin, bile acids, and drugs, J. Clin. Investig. 120 (2010) 2942–2952.

[34] M.N. Shaik, B. Hee, H. Wei, R.R. LaBadie, Evaluation of the effect of rifampin on the pharmacokinetics of the Smoothened inhibitor glasdegib in healthy volunteers, Br. J. Clin. Pharmacol. 84 (2018) 1346–1353.
[35] R. Boinpally, N. Gad, S. Gupta, A. Periclou, Influence of CYP3A4 induction/inhibition on the pharmacokinetics of vilazodone in healthy subjects, Clin. Ther. 36 (2014) 1638–1649.
[36] R. Katayama, T. Sakashita, N. Yanagitani, H. Ninomiya, A. Horiike, L. Friboulet, J.F. Gainor, N. Motoi, A. Dobashi, S. Sakata, Y. Tambo, S. Kitazono, S. Sato, S. Koike, A. John Iafrate, M. Mino-Kenudson, Y. Ishikawa, A.T. Shaw, J.A. Engelman, K. Takeuchi, M. Nishio, N. Fujita, P-glycoprotein mediates ceritinib resistance in anaplastic lymphoma kinase-rearranged non-small cell, Lung Cancer 3 (EBioMedicine, 2016,) 54–66.
[37] S. Yoda, J.J. Lin, M.S. Lawrence, B.J. Burke, L. Friboulet, A. Langenbucher, L. Dardaei, K. Prutisto-Chang, I. Dagogo-Jack, S. Timofeevski, H. Hubbeling, J.F. Gainor, L.A. Ferris, A.K. Riley, K.E. Kattermann, D. Timonina, R.S. Heist, A.J. Iafrate, C.H. Benes, J.K. Lennerz, M. Mino-Kenudson, J.A. Engelman, T.W. Johnson, A.N. Hata, A.T. Shaw, Sequential ALK inhibitors can select for lorlatinib-resistant compound ALK mutations in ALK-positive lung cancer, Canc. Discov. 8 (2018) 714–729.
[38] S.C. Tang, J.S. Lagas, N.A. Lankheet, B. Poller, M.J. Hillebrand, H. Rosing, J.H. Beijnen, A.H. Schinkel, Brain accumulation of sunitinib is restricted by P-glycoprotein (ABCB1) and breast cancer resistance protein (ABCG2) and can be enhanced by oral elacridar and sunitinib coadministration, Int. J. Cancer 130 (2012) 223–233.
[39] K. Thanki, R.P. Gangwal, A.T. Sangamwar, S. Jain, Oral delivery of anticancer drugs: challenges and opportunities, J. Controll. Release: Off. J. Controll. Release Soc. 170 (2013) 15–40.
[40] M. Kato, K. Chiba, A. Hisaka, M. Ishigami, M. Kayama, N. Mizuno, Y. Nagata, S. Takakuwa, Y. Tsukamoto, K. Ueda, H. Kusuhara, K. Ito, Y. Sugiyama, The intestinal first-pass metabolism of substrates of CYP3A4 and P-glycoprotein-quantitative analysis based on information from the literature, Drug Metab. Pharmacokinet. 18 (2003) 365–372.
[41] N.R. Budha, A. Frymoyer, G.S. Smelick, J.Y. Jin, M.R. Yago, M.J. Dresser, S.N. Holden, L.Z. Benet, J.A. Ware, Drug absorption interactions between oral targeted anticancer agents and PPIs: is pH-dependent solubility the Achilles heel of targeted therapy? Clin. Pharmacol. Ther. 92 (2012) 203–213.
[42] J. Aisner, Overview of the changing paradigm in cancer treatment: oral chemotherapy, Am. J. Health-System Pharm.: AJHP: Off. J. Am. Soc. Health-Syst. Pharm. 64 (2007) S4–S7.